JOURNAL OF Applied Polymer SCIENCE

Permanent Antistatic Polypropylene Based on Polyethylene Wax/Polypropylene Wax-Grafting Sodium Acrylate

Xiang Xu,[1] Huining Xiao,[2] Yong Guan,[1] Shuzhao Li,[1] Dafu Wei,[1] Anna Zheng[1]

[1]Key Laboratory for Ultrafine Materials of Ministry of Education, School of Materials Science and Engineering, East China University of Science and Technology, Shanghai 200237, China

[2]Department of Chemical Engineering, University of New Brunswick, Fredericton, New Brunswick, Canada E3B 6C1

Correspondence to: A. Zheng (E-mail: zan@ecust.edu.cn)

ABSTRACT: Two types of permanent antistatic agents, polyethylene wax grafted with sodium acrylate (PEW-*g*-AAS) and polypropylene (PP) wax grafted with sodium acrylate (PPW-*g*-AAS), were prepared using a solution grafting method and applied to PP to enhance antistatic properties. The grafting degree was determined using back titration method, and structures were confirmed by Fourier transform infrared spectroscopy. The antistatic properties of PEW-*g*-AAS/PP blends and PPW-*g*-AAS/PP blends were characterized by surface resistivities (ρ_s) and volume resistivities (ρ_v), and a combination of contact angle measurement, scanning electron microscopy, permittivity, and dielectric loss were used to investigate the surface and inner structures of the blends. Results showed that ρ_s and ρ_v of PEW-*g*-AAS/PP blends dropped significantly (four to seven orders of magnitudes) above a critical addition at 10%, where an electrostatic dissipative network formed; PPW-*g*-AAS revealed an inferior antistatic performance than PEW-*g*-AAS due to its better compatibility and smaller content of dispersed phase in the matrix. Furthermore, the antistatic blends treated in 80°C water, 80°C air, and room temperature were investigated, and the results were interpreted from surface energy. Moreover, the addition of antistatic agent had little impact on tensile strength of the PP matrix. © 2012 Wiley Periodicals, Inc. J. Appl. Polym. Sci. 000: 000–000, 2012

KEYWORDS: polypropylene; polyethylene wax; antistatic; surface energy; volume resistivity

Received 7 September 2011; accepted 13 February 2012; published online 00 Month 2012
DOI: 10.1002/app.37524

INTRODUCTION

With the advantages of low density, good mechanical property, heat-resistant quality, and insulativity, polypropylene (PP) is considered as one of the most widely used thermoplastics. However, the prominent insulativity also limits its application or causes some troubles[1–3]: the PP fiber can easily attract dusts and may lead to electric shocks due to the static caused by friction; when producing biaxially oriented polypropylene films, the electric charges are accumulated and thus cause the films to cling together and to be difficult to separate. Nowadays, the PP has been extensively applied in electronics industry, and the static issue has become the key killer to electron device. To overcome these problems, the antistatic PP needs to be developed.

According to the military handbook DOD-HDBK-263, the antistatic material has a surface resistivity greater than 10^9 Ω/sq but not greater than 10^{14} Ω/sq. The industry standards ANSI/Electronic Industries Association (EIA)-541-1988 and ANSI/ESD S541-200 also defined the electrostatic dissipative material having the surface resistivity at 10^5–10^{12} and 10^4–10^{11} Ω/sq, respectively. There are several ways to eliminate the static in the PP products.[4] Generally, surface coating[5–8] and internal antistatic agents are commonly used. For the inner antistatic agents that are more durable than outer antistatic agents, they become major research directions of antistatic agents in plastics. The classical antistatic agents are usually the "soap-like" compounds with a hydrophobic part and a hydrophilic part,[9] such as antistatic agent SP (Cyanamid Company, NJ) and Barquat CME (Baird Chem. Ind., NY). The low-molecular weight agent migrates to the plastic surface and enhances the surface conductivity by attracting a layer of water. Such products are easy to be applied but have some serious drawbacks: they do not give volume conduction beneath the surface and are readily washed out, thus weakening their long-term effectiveness.

Permanent antistatic property is an essential demand in many applications. Commonly, conductive fillers[10] (e.g., carbon blacks,[11,12] metallic fillers,[13] carbon nanotubes,[14,15] or conductive polymers[16–20]) can be a choice to produce the permanent

antistatic materials. Mixed with the PP, these fillers form a percolating, conductive network inside the polymer matrix. Such a system can reach very high conductivity (up to 1 Ω/sq) with long-term effectiveness. However, the optical transparency and the mechanical properties are deteriorated with the addition of the fillers, thus limiting their applications. Because of the drawbacks addressed earlier, it is desirable to find a new type of antistatic system. One of them is the permanent polymeric antistatic agent,[21] which could be based on an ionic conductive polymer (e.g., polyether–polyamide block copolymer). Such a system is permanent and static-dissipative, which offers the advantage of both surface and volume conduction. Up to now, most of the ionic conductive polymers are prepared by polymerization method with tedious procedures and high cost. In our work, a novel type of permanent antistatic agent, nonpolar polymers bearing plenty of polar groups has been prepared with the grafting method. As nonpolar polymers, polyethylene wax (PEW) and polypropylene wax (PPW) not only have low price but also provide excellent compatibility with PP. With respect to polar groups, sodium acrylate has high ionization to provide the ability of static dissipative.

In this work, the graft polymers, PEW-*g*-AAS and PPW-*g*-AAS, were prepared and blended with PP to fabricate antistatic PP samples. The antistatic performance of the blend samples was evaluated by their ρ_s and ρ_v. In addition, the antistatic properties of antistatic PP samples incorporated of PEW-*g*-AAS and PPW-*g*-AAS were compared, and their structures were investigated by means of scanning electron microscopy (SEM), permittivity, and dielectric loss.

EXPERIMENTAL

Materials

PP T1002 was purchased from China Petroleum and Chemical Corp. (Shanghai, China). PEW WE-3 with molecular weight of 3000–5000 and PPW WP-7 with molecular weight of 5000–8000 were from Jinshan Xingxing Plastic Company (Shanghai, China). Acrylic acid (AA) and sodium hydroxide were analytical grade, from Lingfeng Chemical agent limited company (Shanghai, China). Benzoyl peroxide (BPO) was purified by dissolving in chloroform followed by recrystallized in methanol.

Synthesis of Antistatic Agent

PEW or PPW (20 g) was dissolved in 100 mL of xylene (solution A) in a 250-mL four-necked flask, and the temperature was controlled at 100°C by oil bath under nitrogen atmosphere. AA monomer (7.2 g) and BPO (0.5 g) were dissolved in 20 mL of xylene (solution B). Half of the solution B was poured into solution A, and the other half of solution B was dropwise added within 2 h and kept stirring (500 rpm) for 2 h. The resulting solution was precipitated in excess acetone followed by vacuum filtration. The white powder was obtained after vacuum drying and marked as PEW-*g*-AA/PPW-*g*-AA.

About 20 g PEW-*g*-AA/PPW-*g*-AA was dissolved in 100 mL xylene at 100°C, and neutralized by 1.0*N* NaOH, and then precipitated in acetone. The white precipitate was washed with water–acetone (1: 7 v/v) three times and dried in vacuum drying oven. The product was marked as PEW-*g*-AAS/PPW-*g*-AAS.

Characterization of Antistatic Agents

Grafting degree (GD) of sodium acrylate was defined as the weight percentage of sodium acrylate in PEW-*g*-AAS/PPW-*g*-AAS. It is not feasible to detect the amount of sodium acrylate directly, and so the GD was obtained via titrating PEW-*g*-AA/PPW-*g*-AA using the method[22] detailed as follows: 0.5 g purified sample was first dissolved in 50 mL refluxing xylene for 0.5 h, then 20 mL of 0.05 mol L^{-1} NaOH-ethanol solution was added to eliminate the AA, and, finally, 0.1 mol L^{-1} HCl–acetone solution was used to titrate the excessive NaOH, indicated by phenolphthalein. The GD can be calculated by the following equation (2.1):

$$GD = \frac{v(\mathrm{NaOH})c(\mathrm{NaOH}) - v(\mathrm{HCl})c(\mathrm{HCl})}{m} \cdot M(\mathrm{AAS}) \cdot 100\% \quad (2\text{-}1)$$

where v (NaOH) is the volume of NaOH–ethanol solution (L), v (HCl) the volume of HCl–acetone solution (L), c (NaOH) the concentration of NaOH–ethanol solution (mol L^{-1}), c (HCl) the concentration of HCl–acetone solution (mol L^{-1}), m the mass of sample (g), and M (AAS) the molecular weight of sodium acrylate (mol L^{-1}).

The structure of antistatic agent was characterized by Fourier transform infrared spectroscopy, Nicolet 5700 infrared spectrometer (Thermo Electron Scientific Instruments Corp., LLC, Fitchburg). Melting point was obtained from modulated DSC2910 (TA Instruments Corp., New Castle). The antistatic agent was pressed using a hot press model to form a thin sheet ($160 \times 180 \times 1$ mm^3), and the intrinsic volume resistivity was tested using a ZC-36 resistance meter (Shanghai Precision Instruments Co., China) according to GB/T1410-1989.

Preparation of Antistatic PP Samples

Melt Blending. Polypropylene (PP), antistatic agent, and antioxygen 1010 (0.2 wt %) were mixed in torque rheometer (Polylab RC 300P, Thermo Hakke Co., USA) under the condition of 180°C, 60 rpm for 5 min.

Molding. The blend was molded in a $160 \times 180 \times 1$ mm^3 die first with the hot press, setting the condition of 180°C, 7.5 MPa for 5 min, followed by cold pressing at room temperature, 10 MPa for 5 min. The obtained sample was equally cut into four parts for testing.

Measurements of Antistatic PP Samples

Surface resistivity and volume resistivity were tested using a ZC-36 high-resistance meter. Test condition was 23°C, relative humidity 65% (65% RH), and 500 V voltage, which was referred to GB/T1410-1989.

Permittivity and dielectric loss tan δ were detected using a broadband dielectric spectrometer, Concept 4 (Novocontrol Technologies GmbH & Co. KG, Berod, Germany).

SEM images of cryogenically fractured surfaces were taken by the JSM-6360LV (JEOL, Ltd., Tokyo, Japan) at an accelerating voltage of 20 kV. The SEM samples were gold-sputtered before observation.

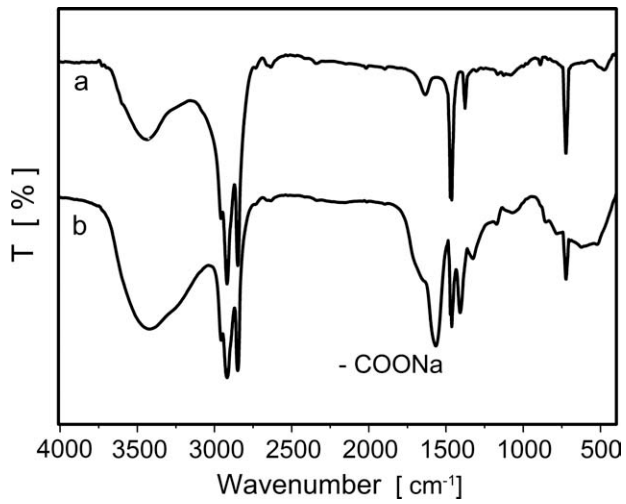

Figure 1. Fourier transform infrared spectroscopy spectra of (a) PEW and (b) PEW-*g*-AAS.

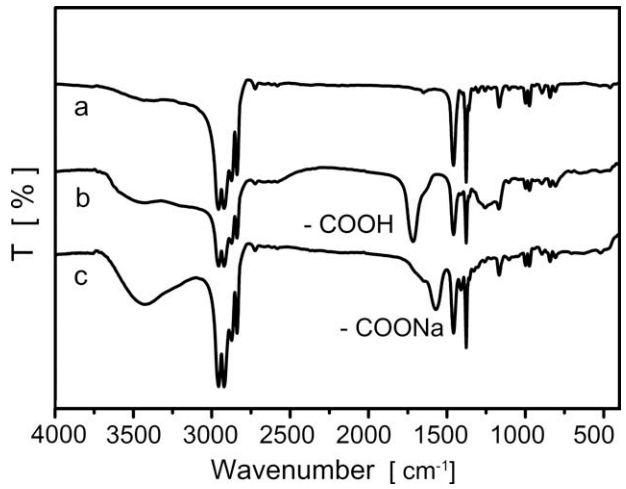

Figure 2. Fourier transform infrared spectroscopy spectra of (a) PPW, (b) PPW-*g*-AA, and (c) PPW-*g*-AAS.

Surface energy was calculated via harmonic mean method[23] in which water contact angle and diiodomethane contact angle were measured by JC2000D (Shanghai Powereach Corp., Shanghai, China) contact angle measuring device.

Tensile tests were conducted using an electronic universal testing machine CMT-400. Tensile samples were prepared via the compression molding according to sample I, GB/T 1040-92. The rate of tensile was set at 5 mm/min. Melting index was measured using a melt flow index meter at 230°C, with 2.16 kg of loading.

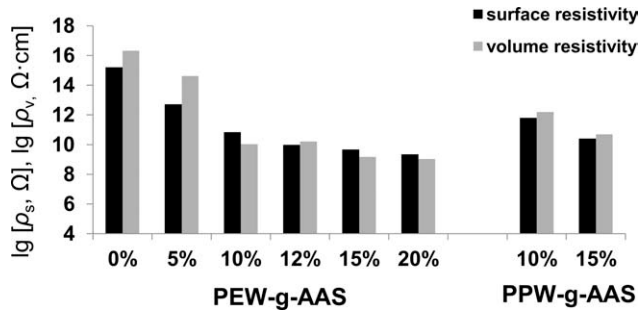

Figure 3. Surface resistivity and volume resistivity of wax/PP samples with different amount of antistatic agent.

RESULTS AND DISCUSSION

Characterization of Antistatic Agents

Sodium acrylate is successfully grafted on PEW chain, which is demonstrated from FTIR results shown in Figure 1. The peaks at 2910, 2840, 1460, and 711 cm^{-1} belong to —CH_2— of PEW, and a new peak at 1570 cm^{-1}, the characteristic absorption peak of sodium carboxylate, appears after grafting. In Figure 2, a new peak at 1710 cm^{-1} corresponds to —COOH of carboxylic acid in PPW-*g*-AA, and the absorption peak moves to 1570 cm^{-1} after neutralization, which confirms the existence of sodium acrylate in the PPW-*g*-AAS.

Table I shows the physical properties of PEW, PPW, and their grafted products. As can be seen, PEW-*g*-AAS displays a lower melting point, 52.0°C, compared to PEW, 103–105.9°C; the reason is investigated by X-ray diffraction, demonstrating that the reduction of the melt point is due to the decrease of the average grain size before and after grafting. Both PEW-*g*-AAS and PPW-*g*-AAS have a dramatic decrease on volume resistivity compared to PEW and PPW.

The GDs of sodium acrylate are 10.6 and 15.4% on PEW and PPW, respectively. It is well known that the GD is often less than 10% for polar monomers to graft on PP/PE using conventional approaches (e.g., melt grafting).[24–27] The high GD should be accounted for the lower viscosity of the melt PEW/PPW.

The Antistatic Effects of PEW-*g*-AAS/PP, PPW-*g*-AAS/PP Composites

Figure 3 shows the surface resistivity and volume resistivity of PEW-*g*-AAS/PP, PPW-*g*-AAS/PP composites with different amounts of PEW-*g*-AAS (or PPW-*g*-AAS). As shown, the control sample (without antistatic agent) has high-surface resistivity (log ρ_s = 15.2 Ω) and volume resistivity (log ρ_v = 16.33 Ω

Table I. The Properties of PEW, PPW and Their Grafts

Agent	Grafting degree (%)	Melt point (°C)	Volume resistivity (Ω cm^{-1})	Appearance
PEW	-	103–105.9	$>10^{14}$	Small white particle
PPW	-	147–151.9	$>10^{14}$	Small particle, light yellow
PEW-*g*-AAS	10.6	52.0	10^5	White power
PPW-*g*-AAS	15.4	147.8	10^6	White power

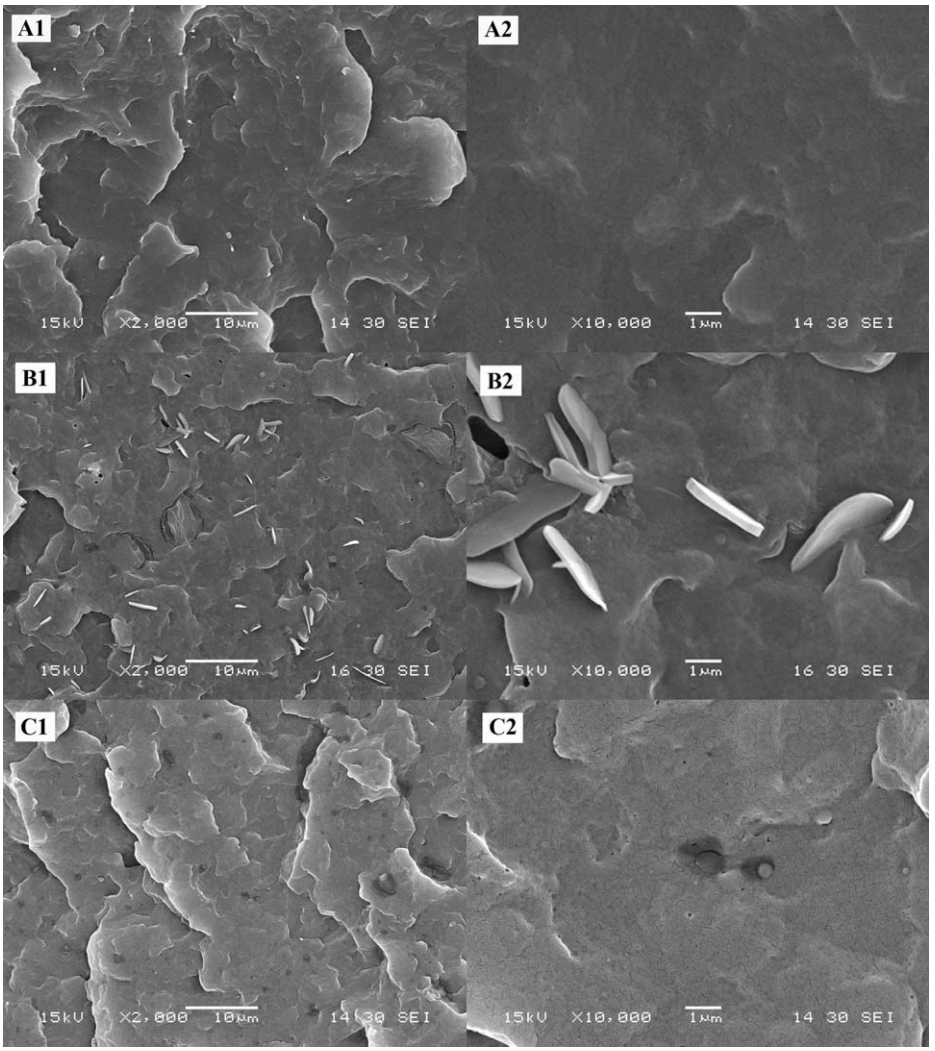

Figure 4. SEM images of fracture sections of PP with/without antistatic agents: A1 pure PP sample, 2000 magnifying power, A2 pure PP sample, 10,000 magnifying power, B1 10% PEW-*g*-AAS sample, 2000 magnifying power, B2 10% PEW-*g*-AAS sample, 10,000 magnifying power, C1 10% PPW-*g*-AAS sample, 2000 magnifying power, C2 10% PPW-*g*-AAS sample, 10,000 magnifying power.

cm). The samples with PEW-*g*-AAS or PPW-*g*-AAS reveal low-surface resistivity (log ρ_s = 9.34–11.8 Ω) and volume resistivity (log ρ_v = 9.03–12.2 Ω cm) when the content of AAS is much more than 10%. As a result, the modified waxes/PP blends meet the criteria for antistatic materials, according to ASTM norm D257-93 and EIA Standard 541. In addition, two phenomena

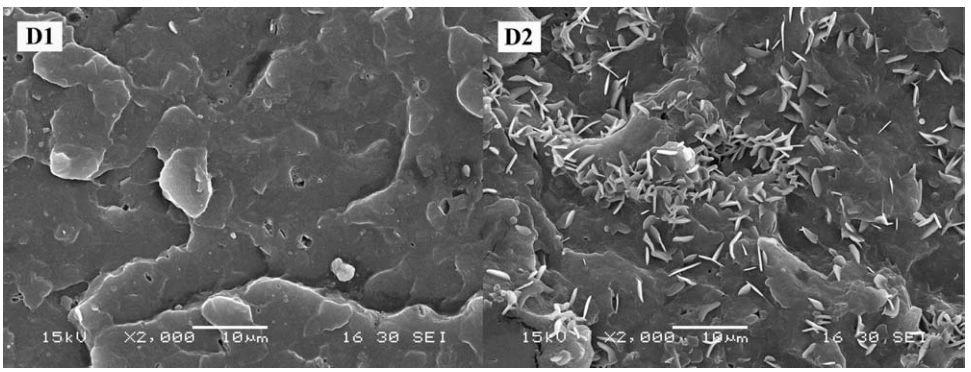

Figure 5. SEM images of PEW-*g*-AAS samples with different contents: D1 5% PEW-*g*-AAS sample, 2000 magnifying power, D2 20% PEW-*g*-AAS sample, 2000 magnifying power.

can be found from Figure 3: (1) while adding same amount of antistatic agent, the samples contained PEW-*g*-AAS exhibit superiority to that with PPW-*g*-AAS. For example, sample (10% PEW-*g*-AAS) has surface resistivity of log ρ_s = 10.84 Ω and volume resistivity of log ρ_v = 10.03 Ω cm, whereas sample (10% PPW-*g*-AAS) has surface and volume resistivity of log ρ_s = 11.8 Ω cm and log ρ_v = 12.2 Ω cm, respectively. (2) For PEW-*g*-AAS/PP composites, low content of PEW-*g*-AAS reveals limited effect on the volume resistivity. However, there is an abrupt drop, nearly four magnitudes, when the content goes up to 10%. After that, the volume resistivity of the composites does not change significantly even though the content goes up to 20%.

Structures of the PEW-*g*-AAS/PP, PPW-*g*-AAS/PP Composites

The microcosmic structures of the composites were investigated by SEM (see Figure 4). The images A1 and A2 are the cross-section of pure PP sample with different magnifications (2000 and 10,000), which show a smooth and uniform surface. From images B1 and B2, PEW-*g*-AAS is scattered into round microsheets in PP matrix, which are about 2–3 μm in diameter and 0.2–0.4 μm in thickness. In contrast, PPW-*g*-AAS has better compatibility with PP matrix, which was dispersed into microbeads with diameter less than 0.1 μm (see images C1 and C2 in Figure 6). This might be due to the fact that PPW-*g*-AAS owns the same repeated unit $-\left(CH_2CH(CH_3)\right)_n-$ with PP, leading to excellent compatibility with the matrix. However, it is easier for the sheets to entangle each other and to form electronic leaking networks than the beads. That is why samples contained PEW-*g*-AAS has better antistatic effect than samples contained PPW-*g*-AAS at the same content.

Sample containing 5% PEW-*g*-AAS shows high-volume resistivity of log ρ_v = 14.46 Ω cm in that the antistatic agent could not form a continuous conducting network structure in the matrix. From the literature study,[11] the conductive properties of a composite are determined by three main factors: (1) specific properties of the components, (2) their relative spatial distribution, and (3) interparticle "contact" resistance between the conductive component. In PP/PEW-*g*-AAS composite, PEW-*g*-AAS has volume resistivity of 10^5 Ω cm, which can be regarded as "conductive" filler in the PP matrix. To dissipate the electrostatic charges, a continuous conducting network is indispensable in the surface or even in the body of the matrix. When a small amount of PEW-*g*-AAS was added, the microsheets were separated, and the electrostatic charges could not be transferred, thus creating a high-volume resistivity as shown in Figure 5(D1). With the increasing of PEW-*g*-AAS, the microsheets began to contact each other, and when a critical threshold was reached, a continuous conducting network was formed eventually, causing an abrupt drop of conductivity. For sample 20% PEW-*g*-AAS, the addition of more PEW-*g*-AAS would enrich the network, as shown in Figure 5(D2), whereas the volume resistivity did not change significantly compared to samples 10% PEW-*g*-AAS and 15% PEW-*g*-AAS.

Permittivity and Dielectric Loss tan *δ*

Figure 6 displays plots of the permittivity ε′ and dielectric loss tan *δ* versus frequency for the PEW-*g*-AAS/PP composites with

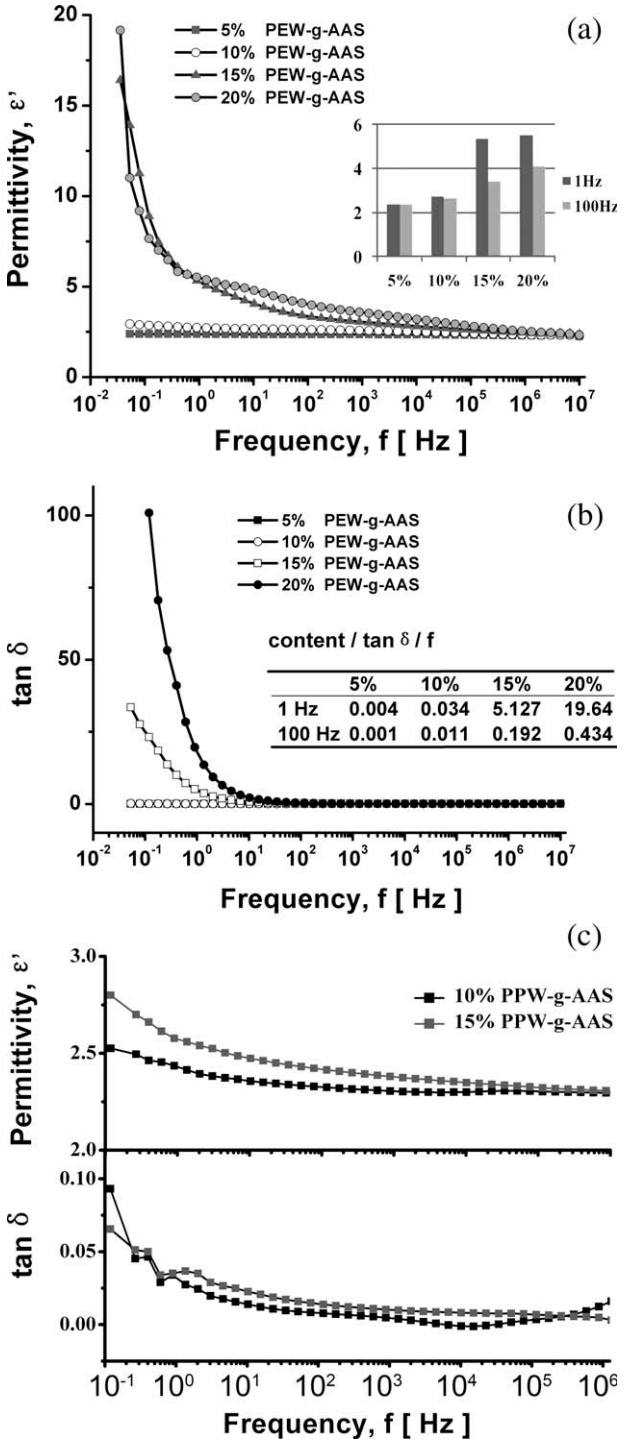

Figure 6. (a) ε′ of PEW-*g*-AAS/PP, (b) tan *δ* of PEW-*g*-AAS/PP, and (c) ε′ and tan *δ* of PPW-*g*-AAS/PP.

various contents of PEW-*g*-AAS at 25°C. As shown, a pronounced drop in ε′ can be observed in the low frequency (<1 Hz) when the content of PEW-*g*-AAS is 15or 20%, after which the decrease becomes temperate till the high frequency (10^7 Hz). In contrast, the e? for 5or 10% sample, which is lower than 15and 20% sample, reveals a slight decrease in the broadband. Similar trends can be found in dielectric loss tan *δ*,

Table II. Surface Resistivity[a] of Wax/PP Composites with Different Treatments/log(ρ_s, Ω)

	Treatment conditions (first day)			Treatment conditions (14th day)		
Antistatic agent (wt %)	Untreated	80°C water 1 h	80°C air 1 h	Untreated	80°C water 1 h	80°C air 1 h
5 (PEW-*g*-AAS)	12.7	11.4	12.8	13.6	10.3	11.1
10 (PEW-*g*-AAS)	10.8	8.2	11.4	11.2	8.9	10.2
15 (PEW-*g*-AAS)	9.7	7.7	12.2	10.3	8.2	9.9
20 (PEW-*g*-AAS)	9.3	7.2	11.9	9.7	8.1	9.7
10 (PPW-*g*-AAS)	11.8	9.2	12.0	12.2	10.3	10.7
15 (PPW-*g*-AAS)	10.4	8.1	11.7	10.8	9.5	10.1

[a]Test condition: 23°C, 65% RH.

shown in (b) of Figure 6. Deserved to be mentioned, the dielectric loss of 15and 20% samples drastically increases with decreasing frequency (<10 Hz). For example, tan δ of 20% sample in 1 Hz is 19.6, which is 45 times of the value in 100 Hz, 0.434. These features can be account for Maxwell–Wagner effect,[28] which demonstrates anomalous dispersion of the materials. The prominent dielectric loss, located below 10 Hz, can be the proof of interfacial polarization, which is induced through a local accumulation of free charges captured by defects or interfaces in the composites. Moreover, PEW-*g*-AAS contains plenty of charge carriers, which cause conduction loss under the external electric field.[29,30]

Comparing with PEW-*g*-AAS/PP, PPW-*g*-AAS/PP composites show limited change in the broadband. This can demonstrate that PPW-*g*-AAS has better compatibility with PP matrix and interfacial polarization weakens tremendously.

Antistatic Effects with Different Treatments

Table II presents the surface resistivity of PEW-*g*-AAS/PP and PPW-*g*-AAS/PP composites: untreated, treated in 80°C water for 1 h, and 80°C air for 1 h. Compared to the untreated samples, the surface resistivity was dropped two magnitudes after treating in 80°C water for 1 h, while increased one to three magnitudes after treating in 80°C air for 1 h. Then the samples were stored in room temperature with 65% RH. Two weeks later, the untreated and water-treated samples showed a little increase in the surface resistivity, while the air-treated samples displayed a considerable drop.

Table III. Water Contact Angle and Diiodomethane Contact Angle of Samples (°)

		Contact angle	
Sample	Antistatic agent (wt %)	Water	Diiodomethane
1	0	94.0	58.7
2	5 (PEW-*g*-AAS)	106.3	63.0
3	10 (PEW-*g*-AAS)	105.5	63.3
4	15 (PEW-*g*-AAS)	104.6	61.1
5	20 (PEW-*g*-AAS)	103.1	59.1
6	10 (PPW-*g*-AAS)	98.3	56.0
7	15 (PPW-*g*-AAS)	91.1	56.8

To explore the reasons why the surface resistivity changed, the surface properties of the samples were investigated. Table III shows the water contact angle and diiodomethane contact angle of PEW-*g*-AAS/PP, PPW-*g*-AAS/PP, and control PP sample. The surface energy is calculated via a harmonic-mean method.[23]

Surface tension is composed of dispersion force σ^d and polar force σ^p:

$$\sigma = \sigma^d + \sigma^p \tag{3-1}$$

According to harmonic-mean equation:

$$\sigma_{SL} = \sigma_S + \sigma_L - \frac{4\sigma_S^d\sigma_L^d}{\sigma_S^d + \sigma_L^d} - \frac{4\sigma_S^p\sigma_L^p}{\sigma_S^p + \sigma_L^p} \tag{3-2}$$

where S stands for solid and L stands for liquid.

Combined with Young equation:

$$\sigma_S = \sigma_{SL} + \sigma_L \cos\theta \tag{3-3}$$

θ is the contact angle.

An expression is obtained:

$$\sigma_L(1 + \cos\theta) = \frac{4\sigma_S^d\sigma_L^d}{\sigma_S^d + \sigma_L^d} + \frac{4\sigma_S^p\sigma_L^p}{\sigma_S^p + \sigma_L^p} \tag{3-4}$$

The dispersion force σ_S^d and polar force σ_S^p of the samples can be calculated using eq. (3-4) by measuring the contact angles of two types of known liquid, water, and diiodomethane. The surface energy σ is also acquired by eq. (3-1), as is shown in Table IV.

Comparing with pure PP, all the samples contained PEW-*g*-AAS have a higher contact angles and lower surface energy, for the surface energy of PE being lower than that of PP. Moreover, the proportion of the dispersion force is more prominent. This demonstrates the PEW-*g*-AAS on the surface takes on a particular morphology: the polar group (—COONa) tends to migrate inward while the hydrophobic part (PEW) is apt to distribute on the surface, in accordance with the lowest energy principle. When the samples were exposed in air, the migration of the polar group resulted in the increase of the surface resistivity, and this process was accelerated in high temperature as the mobility

Table IV. Dispersion Force σ_S^d, Polar Force σ_S^p, and Surface Energy σ of Samples[a]

Antistatic agent (wt %)	σ_S^d ($\times 10^{-3}$ N/m)	σ_S^p ($\times 10^{-3}$ N/m)	σ ($\times 10^{-3}$ N/m)
0	27.8	1.7	29.5
5 (PEW-*g*-AAS)	27.1	0.1	27.2
10 (PEW-*g*-AAS)	26.8	0.1	26.9
15 (PEW-*g*-AAS)	28.1	0.1	28.2
20 (PEW-*g*-AAS)	29.1	0.2	29.3
10 (PPW-*g*-AAS)	30.3	0.6	30.9
15 (PPW-*g*-AAS)	28.7	2.1	30.8

[a] σ_L^d, σ_L^p, and σ_L of water are 21.8 $\times$ 10^{-3} N/m, 51.0 $\times$ 10^{-3} N/m, and 72.8 $\times$ 10^{-3} N/m; for diiodomethane, they are 49.5 $\times$ 10^{-3} N/m, 1.3 $\times$ 10^{-3} N/m, and 50.8 $\times$ 10^{-3} N/m.

of molecules was enhanced. Additionally, high temperature also led to the enrichment of PEW-*g*-AAS because of the exclusion of the PP matrix. While the 80°C air-treated samples in the 65% RH environment, a part of polar groups migrated to the surface causing a considerable drop of surface resistivity. When the samples were contacted with water, the polar group preferred to migrate outward, thus causing the decrease of surface resistivity of samples as shown in Table II.

For PPW-*g*-AAS/PP samples, the surface energies were approximate to that of control PP sample, in that PPW and PP had the same repeated unit.

Different from the traditional antistatic agents, the low-surface energies demonstrated that the ion conduction is the major mechanism to dissipate the static, instead of a water film attracted by the antistatic agents on the surface.

Thermal Behavior and Mechanical Properties of Antistatic Samples

Table V lists the tensile strength and melt index of the antistatic samples along with the controlled sample, PP. The tensile strength decreased slightly for PEW-*g*-AAS samples but was kept almost same for PPW-*g*-AAS because of the better compatibility of PPW-*g*-AAS with PP matrix. For PEW-*g*-AAS samples, the melt index increased with the content of antistatic agent rising. As the molecular weights of PEW-*g*-AAS and PPW-*g*-AAS are much lower than that of PP, the antistatic agent acts as a plasticizer in the blends and hence improves the flowability of plastic.

CONCLUSIONS

Two types of permanent antistatic agents, PEW-*g*-AAS and PPW-*g*-AAS, were successfully prepared via the solution grafting; and the GDs were 10.6and 15.4%, respectively, determined by back titration. The volume resistivity of PEW-*g*-AAS/PPW-*g*-AAS reached a value of $10^5/10^6$ Ω cm. Comparing with PP, PEW-*g*-AAS/PP and PPW-*g*-AAS/PP presented an improved antistatic property: the surface and volume resistivities were dropped to log ρ_s = 9.67 Ω/log ρ_s = 10.4 Ω and log ρ_v = 9.17 Ω cm/log ρ_v = 10.69 Ω cm, respectively, when 15% PEW-*g*-AAS/PPW-*g*-AAS was added. Treated in 80°C water for 1 h, the surface resistivity drops approximately two magnitudes, while treated in 80°C air for 1 h, the surface resistivity increases one to three magnitudes. The SEM, permittivity, and dielectric loss were applied to investigate the compatibility of the composites, which demonstrate that PEW-*g*-AAS was scattered into microsheets and dispersed in PP matrix uniformly, forming a continuous conductive network when the content of modified waxes reached to 10% or higher. In contrast, PPW-*g*-AAS was aggregated into small beads and showed inferior antistatic effect than PEW-*g*-AAS. The addition of the antistatic agent decreased the tensile strength of the blends slightly, and the surface energy was maintained unchanged.

Table V. Tensile Strength and Melt Index of Antistatic Samples

Sample	Tensile strength (MPa)	Melt index (g/10 min)
Pure PP	31.9	2.83
PEW-*g*-AAS 10%	27.55	3.47
PEW-*g*-AAS 15%	26.2	4.01
PEW-*g*-AAS 20%	25.4	5.35
PPW-*g*-AAS 15%	30.39	3.95

ACKNOWLEDGMENTS

The research was supported by Shanghai Leading Academic Discipline Project (B502) and Shanghai Key Laboratory Project (08DZ2230500).

REFERENCES

1. Maki, N.; Nakano, S.; Sasaki, H. *Packag. Technol. Sci.* **2004,** *17*, 249.
2. Dudler, V.; Grob, M. C.; Mérian, D. *Polym. Degrad. Stab.* **2000,** *68*, 373.
3. Kobayashi, T.; Wood, B. A.; Takemura, A.; Ono, H. *J. Electrostat.* **2006,** *64*, 377.
4. Zhao, Z. Q.; Zhang, X. L. The Technology Application of the Conductive and Antistatic Polymer Materials. China Textile and Apparel Press: Beijing, **2006.**
5. Soto-Oviedo, M. A.; Araújo, O. A.; Faez, R.; Rezende, M. C.; Paoli, M. D. *Synth. Met.* **2006,** *156*, 1249.
6. Haas, K. H.; Amberg-Schwab, S.; Rose, K.; Schottner, G. *Surf. Coat. Technol.* **1999,** *111*, 72.
7. Sittinger, V.; Pflug, A.; Werner, W.; Rickers, C.; Vergöhl, M.; Kaiser, A.; Szyszka, B. *Thin Solid Films* **2006,** *502*, 175.
8. Kima, H. K.; Kimb, Y. B.; Choa, J. D.; Honga, J. W. *Prog. Org. Coat.* **2003,** *48*, 34.
9. Ding, Y. S.; Tang, H. O.; Zhang, X. M.; Wu, S. Y.; Xiong, R. Y. *Eur. Polym. J.* **2008,** *44*, 1247.
10. Valentini, L.; Bon, S. B.; Kenny, J. M. *Carbon* **2007,** *45*, 2685.
11. Wycisk, R.; Pozniak, R.; Pasternak, A. *J. Electrostat.* **2002,** *56*, 55.
12. Aal, N. A.; Tantawy, F. E.; Al-Hajry, A.; Bououdina, M. *Polym. Compos.* **2008, 125.**

13. Krupa, I.; Miková, G.; Novák, I.; Janigová, I.; Nógellová, Z.; Lednický, F.; Prokeš, J. *Eur. Polym. J.* **2007,** *43*, 2401.
14. Rhodes, S. M.; Higgins, B.; Xu, Y. J.; Brittain, W. J. *Polymer* **2007,** *48*, 1500.
15. Li, C. S.; Liang, T. X.; Lu, W. Z.; Tang, C. H.; Hu, X. Q.; Cao, M. S.; Liang, J. *Compos. Sci. Technol.* **2004,** *64*, 2089.
16. Martins, C. R.; Paoli, M. D. *Eur. Polym. J.* **2005,** *41*, 2867.
17. Omastová, M.; Chodák, I.; Pionteck, J. *Synth. Met.* **1999,** *102*, 1251.
18. Omastová, M.; Košina, S.; Pionteck, J.; Janke, A.; Pavlinec, J. *Synth. Met.* **1996,** *81*, 49.
19. Omastová, M.; Pavlinec, J. *Polym. Int.* **1997,** *43*, 109.
20. Yang, J. P.; Yang, Y. J.; Hou, J. N.; Zhang, X.; Zhu, W.; Xu, M. *Polymer* **1996,** *37*, 793.
21. Hausmann, K. *Plast. Addict. Com.* **2007,** *3*, 40.
22. Zhu, L. C.; Tang, G. B.; Shi, Q.; Cai, C. L.; Yin, J. H. *React. Funct. Polym.* **2006,** *66*, 984.
23. Hu, F. Z.; Zheng, A. N.; Zhang, Q. A. Polymers and Interface of Their Interface. China Light Industry Press: Beijing, **2001; p 63.**
24. Xiao, H. W.; Yu, F. Y.; Yu, Y.; Huang, S. Q. *J. Appl. Polym. Sci.* **2007,** *104*, 2515.
25. Wong, B.; Baker, W. E. *Polymer* **1997,** *38*, 2781.
26. Chen, H. J.; Shi, X. H.; Zhu, Y. F.; Zhang, Y.; Xu, J. R. *Appl. Surf. Sci.* **2008,** *254*, 2521.
27. Kaneko, H.; Saito, J.; Kawahara, N.; Matsuo, S.; Matsugi, T.; Kashiwa, N. *Polymer* **2008,** *49*, 4576.
28. Dimitry, O. H.; Sayed, W. M.; Mazroua, A. M.; Saad, A. L. G. *Polimero* **2009,** *54*, 8.
29. Rozik, N. N.; Abd-El Messieh, S. L.; Abd-El Nour, K. N. *J. Appl. Polym. Sci.* **2010,** *115*, 1732.
30. Abd-El Messieh, S. L.; Rozik, N. N. *J. Appl. Polym. Sci.* **2011,** *122*, 714.